Microwave Measurements and Calculations for The Glyoxylic Acid - Formic Acid Hydrogen-Bonded

Complex

Jack L. Nichols, Kristen K. Roehling, Adam M. Daly, Stephen G. Kukolicha

Department of Chemistry and Biochemistry, University of Arizona

1306 E. University Avenue, Tucson AZ 85721

Abstract

The gas-phase doubly hydrogen-bonded glyoxylic acid - formic acid hydrogen-bonded complex was obtained by mixing a heated sample of glyoxylic acid with room-temperature formic acid in argon. High-level DFT and MP2 calculations with various basis sets were performed and the structures and rotational constants were determined for the lowest energy dimers of glyoxylic acid - formic acid. The microwave spectrum was measured in the 6-12 GHz frequency range using two Flygare-Balle type pulsed beam Fourier transform microwave (FTMW) spectrometers.

The rotational constants were determined to have the following values: A = 5533.911(3), B = 923.3883 (5), and C = 792.1132(6) MHz using 18 transitions. B3LYP/ cc-pVQZ calculations for the lowest energy dimer yielded calculated rotational constants of A = 5551.2, B = 922.9 and C = 791.3 MHz.

<sup>a</sup> kukolich@arizona.edu

1

#### 1. Introduction

We report the first microwave measurements of the gas phase dimer consisting of glyoxylic acid and formic acid. Glyoxylic acid is important in metabolism<sup>1</sup> and other areas of biology. The monomers of glyoxylic acid have been the subject of earlier microwave spectroscopy analysis by Mollendal<sup>2,3,4</sup>. Internal hydrogen bonding affects the stabilization of three known structural isomers. The various conformers are shown in Figure 1. The lowest energy conformer is labeled as trans-1, in Figure 1. The trans-1 structure consistent with their measurements has an internal hydrogen bond from the hydroxyl group to the carbonyl group on carbon atom 2. The trans-2 structure has an internal hydrogen bond in the carboxyl group and was not observed and has been calculated to be 505 cm<sup>-1</sup> higher in energy than trans-1. The first detection of the trans-2 conformer was made using microwave-radio double resonance<sup>5</sup>. To our knowledge, no direct microwave measurements have been made. By viewing the doubly hydrogen bonding complex of glyoxylic acid with formic acid, we continue the investigation into the effect of hydrogen bonding on the structure of glyoxylic acid complexes. The biological activity of glyoxylic acid, combined with the diverse hydrogen bonding possibilities with formic acid, presents an interesting system for using microwave spectroscopy to probe the gas phase structure of the glyoxylic acid—formic acid complex.

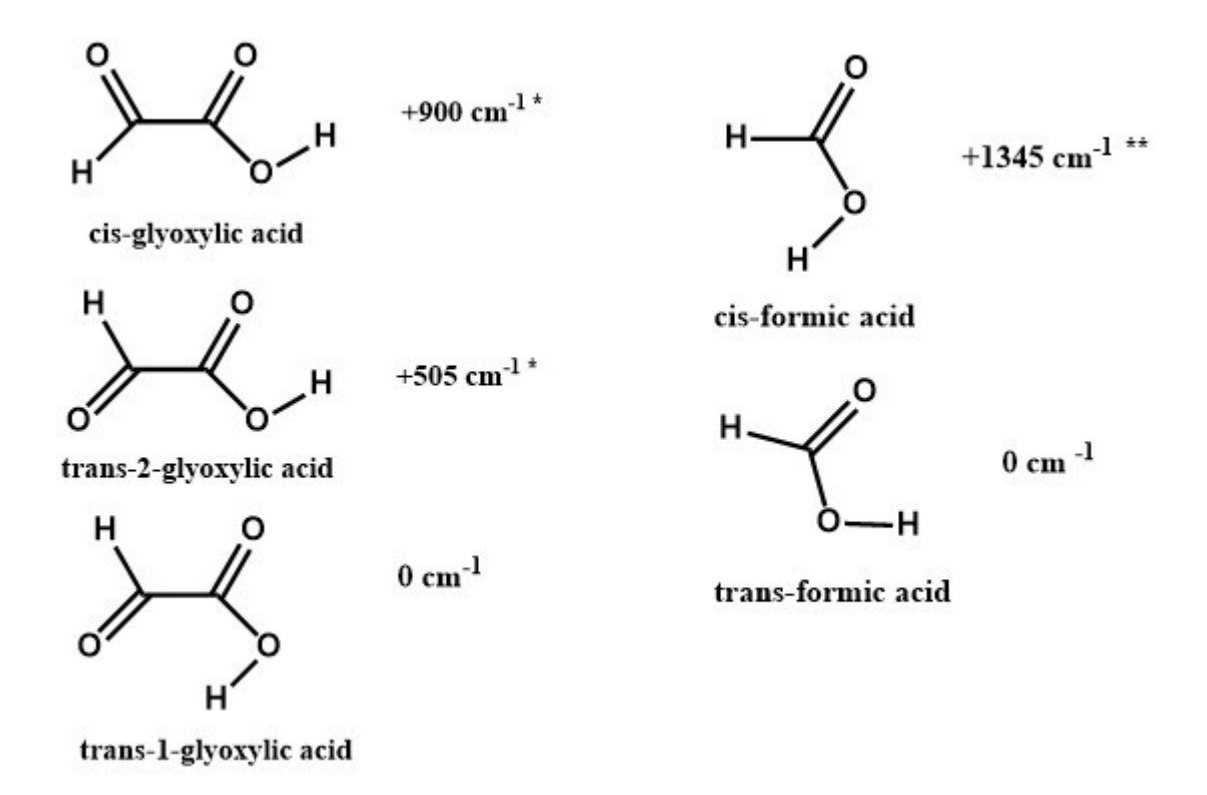
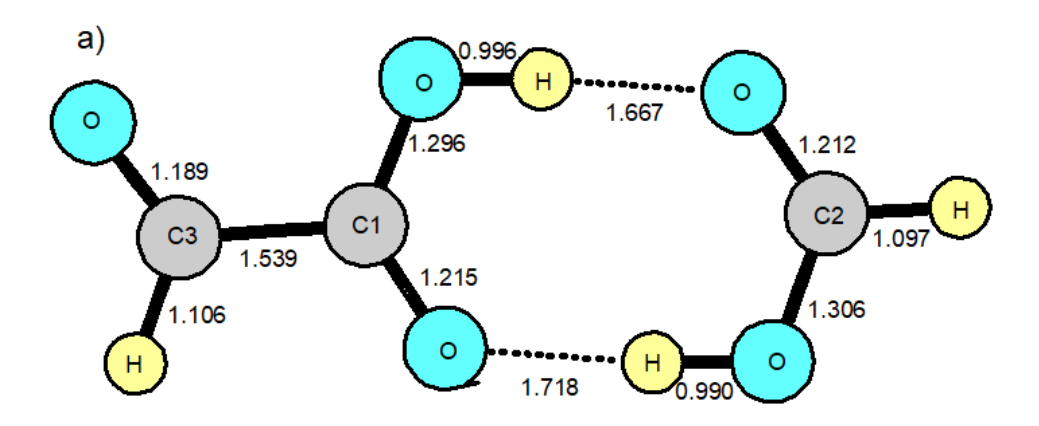


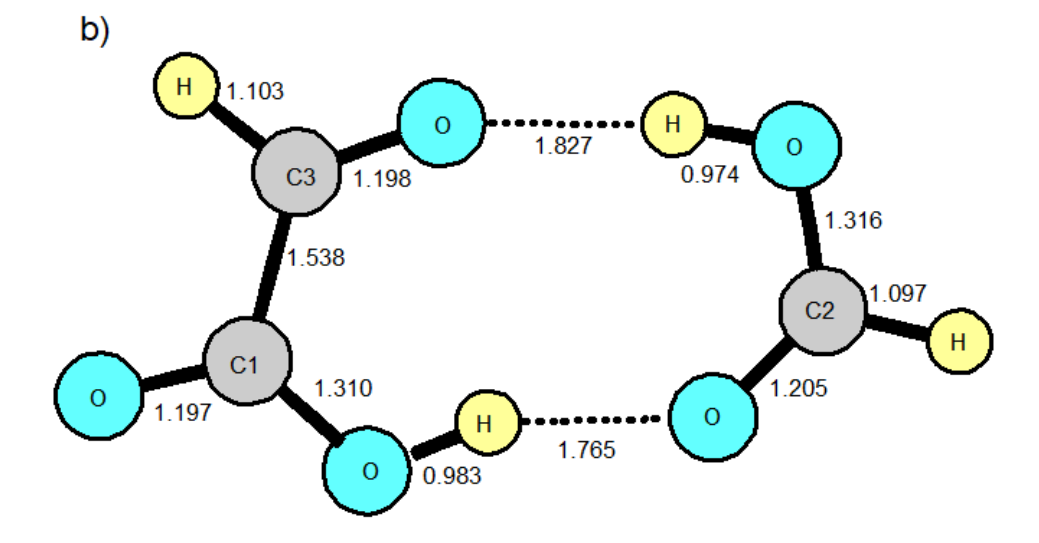
Figure 1. Monomers of Glyoxylic Acid and Formic Acid (\* MP2/cc-pVTZ, \*\* Ref(7)).

Formic acid is the simplest carboxylic acid and has been extensively studied both as a monomer in the trans form<sup>6</sup> (lowest energy) and cis form<sup>7</sup> (+1345 cm<sup>-1</sup>), and as a doubly hydrogen-bonded complex in a variety of dimers in the gas phase. The HCOOH—DCOOH<sup>8</sup> dimer and numerous heterodimers have been shown to exhibit concerted proton tunneling. Examples are: propiolic acid – formic acid,<sup>9,10,11</sup> nitric acid – formic acid<sup>12</sup>, and acetic acid – formic acid<sup>13</sup>. Doubly hydrogen-bonded complexes can provide simple models for hydrogen bonding present in DNA base pairs. Dimers that model the hydrogen bonding in biologically relevant acids have also been studied and examples are, formic acid – ammonia<sup>14</sup>, formic acid – formamide,<sup>15</sup> and maleimide – formic acid<sup>16</sup>.

Doubly hydrogen-bonded structures can be made with trans formic acid with all three of the conformers of glyoxylic acid, the trans-1, trans-2 and cis conformers. The EEa structure is a complex between the trans-2 glyoxylic acid and formic acid. One can form a similar complex by combining cis

glyoxylic acid with formic acid to form the EEb complex. The three possible low-energy, doubly hydrogen-bonded structures are shown in Figure 2.





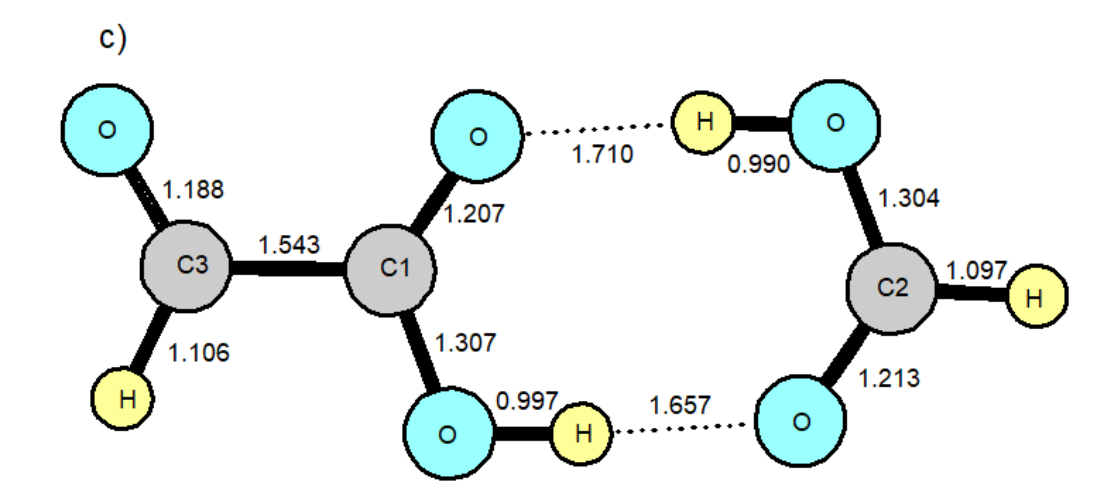


Figure 2. The three lowest energy calculated structures for glyoxylic acid - formic acid dimer. a) is identified as the end-to-end configuration (EEa), b) is the side-by-side configuration (SS) and c) is the second end-to-end configuration (EEb).

## 2. Experimental

Rotational transitions of the glyoxylic acid-formic acid heterodimer in the region of 6-12 GHz were measured using two Flygare-Balle type pulsed-beam Fourier transform microwave spectrometers. One has the molecular beam perpendicular to the cavity axis, and the second has the beam at a 45° angle to the cavity axis and may exhibit Doppler doubling (Figure 3). These instruments, at the University of Arizona, have been previously described 17,18. Measurements of rotational transitions were saved at multiple frequencies using a program that analyzes the results of a fast Fourier transform of a free-induction decay (FID) signal. An example of the recorded spectrum with the stimulating microwave frequency of 6834.27 MHz is given in Figure 3.

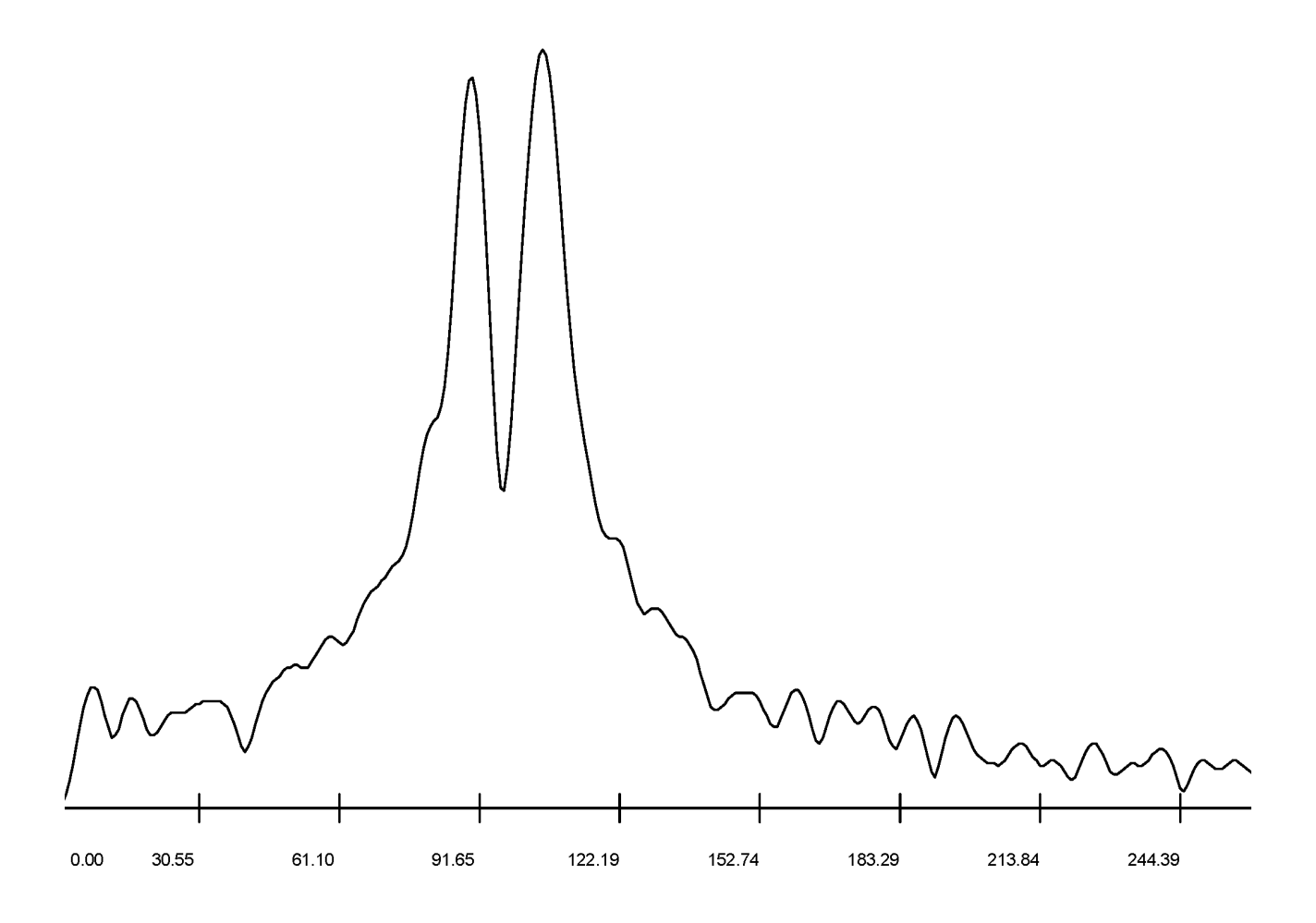


Figure 3. Direct measurement of the  $4_{04} \rightarrow 3_{03}$  transition using a microwave stimulation frequency of 6834.270 MHz. Frequency scale in kHz relative to the stimulating frequency. The molecular signal was recorded at 6834.432 MHz.

Glyoxylic acid monohydrate (98 %) was purchased from Sigma-Aldrich, and it was used without further purification. The glyoxylic acid monohydrate was placed into a glass sample cell, and was heated to 50 °C to produce sufficient vapor pressure. Formic acid (98 %) was purchased from Sigma-Aldrich, and was used without further purification. The formic acid was placed in a separate glass sample cell fitted with a valve that allowed fixed small amounts of formic acid to be added. This sample did not require heating due to its high vapor pressure. The glyoxylic acid monohydrate sample

and formic acid sample were connected through a gas-handling system using argon as the carrier gas. To form the heterodimer of glyoxylic acid-formic acid, the gas-handling system was initially evacuated using a roughing pump. After closing the connection to the pump, the sample cell containing formic acid was opened to the system, allowing formic acid to enter. This sample cell was closed off, and argon was passed into the system to mix with formic acid. Then, the connection to the glyoxylic acid monohydrate sample was opened, and formic acid and argon were allowed to pass over the glyoxylic acid and enter the cavity of the spectrometer. The system was maintained at a backing pressure of 1 atm. The pressure inside the cavity of the instrument was maintained in the range of 10<sup>-6</sup>-10<sup>-7</sup> torr using a diffusion pump. The dimer of glyoxylic acid-formic acid was pulsed into the chamber at a frequency of 2 Hz using a General Valve pulsed valve.

## 3. Computational

Structural parameters, rotational constants and energies were calculated using Gaussian G-16<sup>19</sup> on the University of Arizona HPC system. The calculations were done on the HPC Puma, with 94 cores and 512 GB of memory per node using 268 Gb of memory. Methods used for the calculations below include M11<sup>20</sup>, MP2<sup>21</sup> and B3LYP<sup>22</sup>. The basis sets utilized below are aug-cc-pVQZ<sup>23</sup>, cc-pVQZ<sup>24</sup>, cc-pVDZ<sup>24</sup>, def2-QZVPP<sup>25</sup>, and cc-pVTZ<sup>26</sup>. The experimentally fitted parameters are compared to calculated parameter values for the three potential glyoxylic acid – formic acid structures in Table 1.

The calculated rotational constants and other parameters of interest are provided in Table 1.

Table 1 presents the detailed results of calculations for the three structures, EEa, SS and EEb.

The calculations were initially done to predict the rotational constants to search for lines. The similar results for the various three methods or basis sets for each structure show the consistency of the calculations and help to determine which methods and basis sets are the best for this problem. The

short and concise Table 2 summarizes the total energies obtained using only the B3LYP/cc-pVQZ and MP2/cc-pVQZ methods for all three structures to compare the relative energies. Rotational constants for the low-energy EEa structure shown in Figure 2 were used to search for lines and that calculation (column 2 of Table 1.) provides an excellent fit to the experimental lines (column 1). The energies of the EEa and EEb structures only differ by 162 cm<sup>-1</sup> and the rotational constants are very similar (Table 1 – column 2 – EEa). If concerted proton tunneling were present, these two structures would represent the endpoints (two energy minima) of the tunneling motion. G-16 counterpoise calculations with B3LYP-cc-pVQZ basis yield a binding energy of 6226 cm<sup>-1</sup> for the EEa complex, and a binding energy of 6547 cm<sup>-1</sup> for the EEb complex. This is consistent with the higher energy of the glyoxylic acid monomer in the EEb complex. These counterpoise calculations may not properly account for which glyoxylic acid monomer is in the dissociation products.

Notably, the B3LYP, DFT method with the cc-pVQZ basis set yielded estimates of glyoxylic acid - formic acid rotational constants closest to the experimental B and C values. The MP2 calculation yielded an A value closest to the experimental value. The side-to-side structure shown in Figure 2 has rotational constants much different from experimental values and the energy is higher by 1500 cm<sup>-1</sup>. Lines attributable to this second structure were observed and that will be discussed in another publication.

The calculated structures for trans-2 and trans formic, End-to-End-a (EEa) structure are given in Figure 2 with the trans-1 and trans formic, Side-to-Side (SS) structure. A third structure is possible using cis-glyoxylic acid and trans formic acid, End-to-End-b (EEb), and the results of our calculations are summarized in Table 1. The energies of the potential dimers were compared using MP2 with cc-pVQZ and M11 with def2qzvpp as shown in Table 2. The B3LYP calculations for all three isomers used the same cc-pVQZ basis functions and relative energies are given in cm<sup>-1</sup>.

Table 1. Experimental parameters compared to calculated parameters for three potential dimer structures: EEa, SS, and EEb.

Parame ter	1. Experim ental	2. B3LYP	3. M11	4. MP2	5. B3LYP	6. M11	7. MP2	8. B3LYP	9. M11	10. MP2
Structur e	EEa	EEa	EEa	EEa	SS	SS	SS	EEb	EEb	EEb
Basis set	-	b	а	а	b	С	b	b	С	b
A (MHz)	5533.91 2(3)	5551.2	5653.9	5540.2	4027.9	4248.7	4127.5	5288.6	5272.8	5253.6
B (MHz)	923.388 3(5)	922.9	920.8	929.4	1046.1	1031.4	1039.7	935.0	937	944.3
C (MHz)	792.113 2(6)	791.3	791.9	795.9	830.4	829.9	830.5	794.5	795.6	800.5
μ <sub>a</sub> (Debye)	ı	1.79	1.89	1.78	2.65	2.8	2.57	1.69	1.72	1.67
μ <sub>b</sub> (Debye)	-	1.41	1.51	1.41	2.23	2.4	2.26	1.54	1.71	1.54
Energy (hartree s)	-	- 493.101 9292	- 492.938 7096	- 492.275 495	- 493.095 0949	- 492.947 1571	- 492.251 2757	- 493.101 1892	- 492.952 4612	- 492.257 4788
a. aug-cc-p	a. aug-cc-pVQZ b. cc-pVQZ c. def2qzvpp									

Table 2. Calculated relative energies in cm<sup>-1</sup> between potential dimer structures.

Structure	EEa	EEb	SS
Relative energy with B3LYP/cc-			
pVQZ	0	162	1500
Relative energy with MP2/cc-			
pVQZ	0	152	1513
Relative energy with			
M11/def2qzvpp	0	173	1337

#### 4. Analysis

The initial A, B, and C rotational constants from the predictions in Table 1. were used in Pickett's SPCAT<sup>27</sup> program to predict the a-dipole pure rotational spectrum. Once both monomer signals were observed, wide scans centered on the predicted  $4_{04} \rightarrow 3_{03}$  transition at 6800 MHz were made. Initially, three transitions were observed in the range 6700-6900 MHz. Additional scans were made for the predicted  $4_{14} \rightarrow 3_{13}$  transition at 6500 MHz. Based on the signals observed, a third wide scan was made at 8500 where the predicted  $5_{05} \rightarrow 4_{04}$  transition is centered. Only one signal was observed at a signal-to-noise ratio of 10. Using this transition, a fit using SPFIT with three transitions was created by fixing the rotational constant A to the average of the calculated values obtained using MP2/ cc-pVQZ and M11/ def2qzvpp and a new prediction using SPCAT was made. A narrow scan centered at 7100 MHz where  $4_{13} \rightarrow 3_{12}$  was predicted was performed and a signal was detected at 7118 MHz. The signal was assigned and the four transitions were fit to three rotational constants A, B and C. The fit was able to predict several more signals within kilohertz of the prediction made by the fit. The new transitions were included and through an iterative process, the final fit was made. A total of 18 transitions, 15 a-dipole transitions and 3 b-dipole transitions have been measured. These 18 transitions were initially fit to a rigid rotor Hamiltonian in SPFIT. The inclusion of the distortion constant D<sub>J</sub> was found to improve the fit to experimental uncertainty and was included in the present analysis. The resulting frequencies are shown in Table 3. and the molecular parameters are in Table 4. Molecular parameters are the rotation constants A, B, C and D<sub>J</sub>.

Table 3. Results of the SPFIT least squares fit to measured transitions. The resulting parameters are in Table 4.

$J_{KaKc}'$	$J_{KaKc}^{\prime\prime}$	Measured (MHz)	Obs-calc (kHz)
1 <sub>11</sub>	000	6326.0278	3.4
2 <sub>12</sub>	1 <sub>01</sub>	7910.2474	-1.3
3 <sub>13</sub>	2 <sub>02</sub>	9429.8839	-2.3
4 <sub>04</sub>	3 <sub>03</sub>	6834.4320	6.4
4 <sub>13</sub>	3 <sub>12</sub>	7118.9092	9.0
$4_{14}$	3 <sub>13</sub>	6594.0161	-1.7
4 <sub>23</sub>	3 <sub>22</sub>	6859.8345	-3.5
5 <sub>05</sub>	4 <sub>04</sub>	8522.5703	2.6
5 <sub>14</sub>	4 <sub>13</sub>	8893.1885	6.2
5 <sub>15</sub>	4 <sub>14</sub>	8237.5693	-0.3
5 <sub>23</sub>	4 <sub>22</sub>	8626.2275	-4.3
524	4 <sub>23</sub>	8571.3259	-4.9
6 <sub>06</sub>	5 <sub>05</sub>	10197.5488	-0.6
6 <sub>15</sub>	5 <sub>14</sub>	10663.6317	0.0
6 <sub>16</sub>	5 <sub>15</sub>	9878.0117	-1.9
624	5 <sub>23</sub>	10375.8885	-10.5
7 <sub>07</sub>	6 <sub>06</sub>	11857.5186	-2.0
7 <sub>17</sub>	6 <sub>16</sub>	11514.9248	8.7

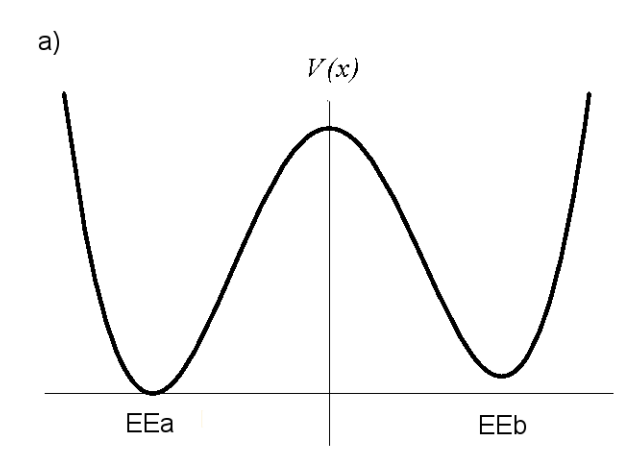
Table 4. The molecular parameters for glyoxylic acid-formic acid dimer from the least squares fit to data in Table 3. 18 transitions were in the fit. The standard deviation for the fit,  $\sigma = 3 \text{ kHz}$ .

A (MHz)	5533.9115(33)
B (MHz)	923.38830(45)
C (MHz)	792.11317(57)
D <sub>J</sub> (kHz)	0.0779(69)
σ (kHz)	3.04

#### 5. Discussion

Using the high-level calculations for the glyoxylic acid-formic acid complex to obtain the two lowest energy structures, a fit has been assigned to the End-to-End-a (EEa) structure. The predicted rotational constants are consistent with the experimentally determined values reported in Table 1. The structure is composed of the second most stable monomer isomer that has not been directly detected experimentally with formic acid. Calculations indicate that the EEa dimer is the lowest energy structure and based on our analysis, the lowest energy dimer of glyoxylic acid and formic acid has been detected. The trans-1 isomer was found by Møllendal<sup>2,3</sup> (et al.) to be more stable than the trans-2 isomer by 5.0(20) kJ/mol, and the trans-1 isomer was also determined to be more stable than the cis isomer. The End-to-End-b (EEb) structure for the complex is predicted to be 162 cm-1 higher in energy and is composed of the cis-glyoxylic acid – trans formic acid dimer. Large scans around predicted transitions for (EEb) have been performed but no successful fit of the transitions consistent with this structure had been made.

Concerted proton tunneling would convert the EEa isomer to the EEb isomer. The potential for this concerted proton tunneling for this dimer would be an asymmetric double-well potential energy as shown in Figure 5. This problem is discussed by Sidorov, et al.<sup>28</sup>



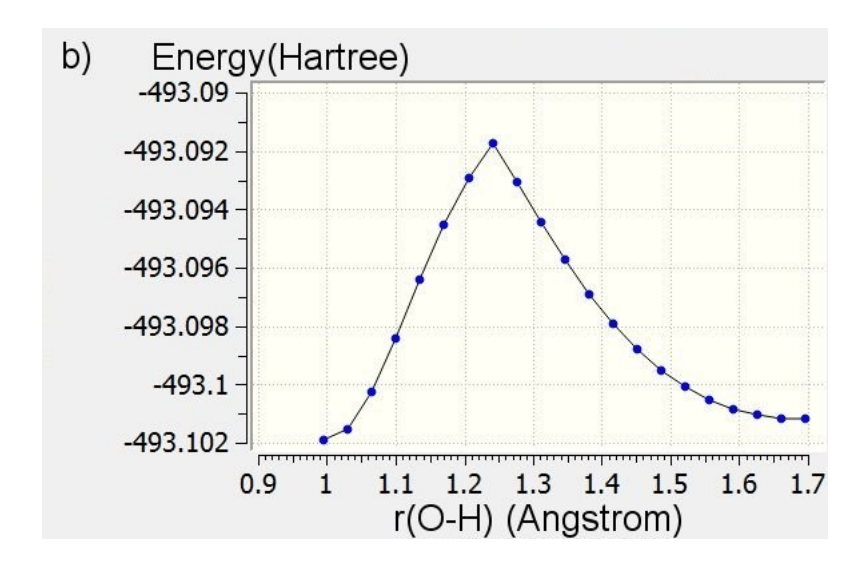


Figure 5. a) Typical asymmetric double-well potential b) Calculated center region of the double - well potential for EEa → EEb using the G-16 scan function. Energy (Hartrees) vs. one O-H bond (Å).

The potential V(x) for this process was calculated using the scan function in G-16 is shown in Figure 5. This was calculated by scanning one O-H bond length and optimizing the structure at each point. This gives a barrier height of approximately 2200 cm<sup>-1</sup>. The asymmetry is an artifact resulting from constant size steps in one O-H bond followed by optimizations.

The lowest energy state would be the sum of functions for EEa and EEb and the next higher state would be the diffference of functions for EEa and EEb, with appropriate coefficients. Tunneling in an asymmetric double well was discussed by by Sidorov, et al.<sup>28</sup> and approximate wavefunctions are given. In the asymmetric double well, the EEa state would be more heavily weighted. If the tunneling splitting is large (>1000cm<sup>-1</sup>) we would only expect to observe the state with the sum linear combination(EEa). This may explain the lack of a separate spectrum for EEb. Tunneling splittings were not observed in other doubly hydrogen-bonded complexes such as formamide-formic acid.<sup>15</sup>

The cis-gloxylic acid monomer has not been experimentally determined but is predicted to form a very low energy dimer (EEb), only 162 cm<sup>-1</sup> higher than the lowest energy dimer (EEa). Although EEb is predicted to be more stable than the Side-to-Side (SS), cis-glyoxylic acid may not be present

in the mixture prior to the expansion and this may be the reason we have not observed signals consistent with this structure.

### 6. Conclusions

The doubly hydrogen-bonded glyoxylic acid - formic acid hydrogen-bonded complex has been investigated using microwave spectroscopy. The structure most consistent with the microwave measurements is the end-to-end structure (EEa) shown in Figure 2. No evidence for a concerted tunneling motion was observed in the spectra. These results should help to understand glyoxylic acid binding with other molecules.

# 7. Acknowledgements

This material is based upon work supported by the National Science Foundation under Grant No. CHE-1952289 at the University of Arizona.

Sb1----

- <sup>9</sup> A.M. Daly, P.R. Bunker, S.G. Kukolich, J. Chem. Phys. 132 (2010) 201101/1–201101/3, https://doi.org/10.1063/1.3443508
- <sup>10</sup> A.M. Daly, P.R. Bunker, S.G. Kukolich, J. Chem. Phys. 133 (2010) 079903/1, https://doi.org/10.1063/1.3472345
- <sup>11</sup> A.M. Daly, K.O. Douglass, L.C. Sarkozy, J.L. Neill, M.T. Muckle, D.P. Zaleski, B.H. Pate, S.G. Kukolich, J. Chem. Phys. 135 (2011) 154304/1–154304/12, https://doi.org/10.1063/1.3643720
- <sup>12</sup> R.B. Mackenzie, C.T. Dewberry, K.R. Leopold, J. Phys. Chem. A 118(36) (2014) 7975-7985. https://doi.org/10.1021/jp507060w
- <sup>13</sup> M.C.D. Tayler, B. Ouyang, B.J. Howard, J. Chem. Phys. 134 (2011) 054316/1–054316/9, https://doi.org/10.1063/1.3528688
- <sup>14</sup> K.K. Roehling, J.L. Nichols, A.M. Daly, and S.G. Kukolich J. Mol. Spectrosc. 393 (2023) 111772. https://doi.org/10.1016/j.jms.2023.111772
- <sup>15</sup> A.M. Daly, B.A. Sargus, S.G. Kukolich J. Chem. Phys. 133 (2010) 174304/1–174304/6. https://doi.org/10.1063/1.3501356
- <sup>16</sup> A.M. Peilovas, and S.G. Kukolich J. Mol. Spectrosc. 321 (2016) 1-4.
- <sup>17</sup> R. E. Bumgarner and S. G. Kukolich, *J. Chem. Phys.* **86** (1987), 1083–1089 https://doi.org/10.1063/1.452248

<sup>&</sup>lt;sup>1</sup> B.A. McFadden, and W.V., Howes,. Anal. Biochem. 1(3) (1960) 240-248. https://doi.org/10.1016/0003-2697(60)90051-8

<sup>&</sup>lt;sup>2</sup> K. M. Marstokk and Mol H. Møllendal, Volume 15, Issue 1, January 1973, Pages 137-150 . J. Mol. Spec., (2001) 208(1), pp.92-100. https://doi.org/10.1016/0022-2860(73)87014-0B.

<sup>&</sup>lt;sup>3</sup> I. Christiansen, K.M. Marstokk, and H. Møllendal, J. Mol. Struct. 30(1) (1976) 137-144. https://doi.org/10.1016/0022-2860(76)85054-5

<sup>&</sup>lt;sup>4</sup> B. Bakri, J. Demaison, L. Margules, and H. Møllendal, . J. Mol. Spectrosc. 208(1) (2001) 92-100. https://doi.org/10.1006/jmsp.2001.8366

<sup>&</sup>lt;sup>5</sup> B.P. Van Eijck, and F.B. van Duineveldt, J. Mol. Struct. 39(2) (1977) 157-163. https://doi.org/10.1016/0022-2860(77)85086-2

<sup>&</sup>lt;sup>6</sup> R.G. Lerner, B.P. Dailey, and J.P. Friend J. Chem. Phys. 26(3) (1957)..680-683

<sup>&</sup>lt;sup>7</sup> W. H. Hocking, 1976.. Z. Naturforsch. A, 31(9) (1976) 1113-1121.

<sup>&</sup>lt;sup>8</sup> W.Li, L. Evangelisti, Q. Gou, W. Caminati, R. Meyer, Angew. Chem., Int. Ed. Engl. 58 (2019) 859-865. <a href="https://doi.org/10.1002/anie.201812754">https://doi.org/10.1002/anie.201812754</a>

- <sup>18</sup> B. S. Tackett, C. Karunatilaka, A. M. Daly, and S. G. Kukolich, *Organometallics* **26** (2007), 2070–2076 https://doi.org/10.1021/om061027
- <sup>19</sup> Gaussian 16, Revision C.01, Frisch, M. J.; Trucks, G. W.; Schlegel, H. B.; Scuseria, G. E.; Robb, M. A.; Cheeseman, J. R.; Scalmani, G.; Barone, V.; Petersson, G. A.; Nakatsuji, H.; Li, X.; Caricato, M.; Marenich, A. V.; Bloino, J.; Janesko, B. G.; Gomperts, R.; Mennucci, B.; Hratchian, H. P.; Ortiz, J. V.; Izmaylov, A. F.; Sonnenberg, J. L.; Williams-Young, D.; Ding, F.; Lipparini, F.; Egidi, F.; Goings, J.; Peng, B.; Petrone, A.; Henderson, T.; Ranasinghe, D.; Zakrzewski, V. G.; Gao, J.; Rega, N.; Zheng, G.; Liang, W.; Hada, M.; Ehara, M.; Toyota, K.; Fukuda, R.; Hasegawa, J.; Ishida, M.; Nakajima, T.; Honda, Y.; Kitao, O.; Nakai, H.; Vreven, T.; Throssell, K.; Montgomery, J. A., Jr.; Peralta, J. E.; Ogliaro, F.; Bearpark, M. J.; Heyd, J. J.; Brothers, E. N.; Kudin, K. N.; Staroverov, V. N.; Keith, T. A.; Kobayashi, R.; Normand, J.; Raghavachari, K.; Rendell, A. P.; Burant, J. C.; Iyengar, S. S.; Tomasi, J.; Cossi, M.; Millam, J. M.; Klene, M.; Adamo, C.; Cammi, R.; Ochterski, J. W.; Martin, R. L.; Morokuma, K.; Farkas, O.; Foresman, J. B.; Fox, D. J. Gaussian, Inc., Wallingford CT, 2016.
- <sup>20</sup> R. Peverati and D. G. Truhlar J. Phys. Chem. Lett. **2** (2011) 2810-2817. DOI: 10.1021/iz201170d
- <sup>21</sup> M. Head-Gordon, J.A. People and M.J. Frisch, Chem. Phys. Lett. 153(6) (1988) 503-506. https://doi.org/10.1016/0009-2614(88)85250-3
- <sup>22</sup> A. D. Becke, J. Chem. Phys. **98** (1993) 5648-52. DOI: 10.1063/1.464913
- <sup>23</sup> R.A. Kendall, T.H. Dunning Jr, and R.J. Harrison J. Chem. Phys. 96(9) (1992) 6796-6806. https://doi.org/10.1063/1.462569
- <sup>24</sup> T.H. Dunning Jr J. Chem. Phys. 90(2) (1989) 1007-1023. https://doi.org/10.1063/1.456153
- <sup>25</sup> F. Weigend, , F. Furche, and R. Ahlrichs J. Chem. Phys. 119(24) (2003) 12753-12762. https://doi.org/10.1063/1.1627293
- <sup>26</sup> T.H. Dunning Jr J. Chem. Phys. 90(2) (1989) 1007-1023. https://doi.org/10.1063/1.456153
- <sup>27</sup> H.M. Pickett. J. Mol. Spectrosc. 148 (1991) 371–377, https://doi.org/10.1016/0022-2852(91)90393-0 <a href="http://spec.jpl.nasa.gov/ftp/pub/calpgm/spinv.html">http://spec.jpl.nasa.gov/ftp/pub/calpgm/spinv.html</a>>
- <sup>28</sup> A. I. Sidorov, B. J. Dalton, S. M. Whitlock, and F. Scharnberg, *Phys. Rev.* A 74, 023612 (2006)